

Dynamic Path Navigation for Motion Agents with LLM Reasoning

Yubo Zhao^{1*} Qi Wu^{1*} Yifan Wang^{1*} Yu-Wing Tai² Chi-Keung Tang¹

¹The Hong Kong University of Science and Technology ²Dartmouth College

{yzhaodx, qwuaz, ywangpa}@connect.ust.hk, yu-wing.tai@dartmouth.edu, cktang@cse.ust.hk

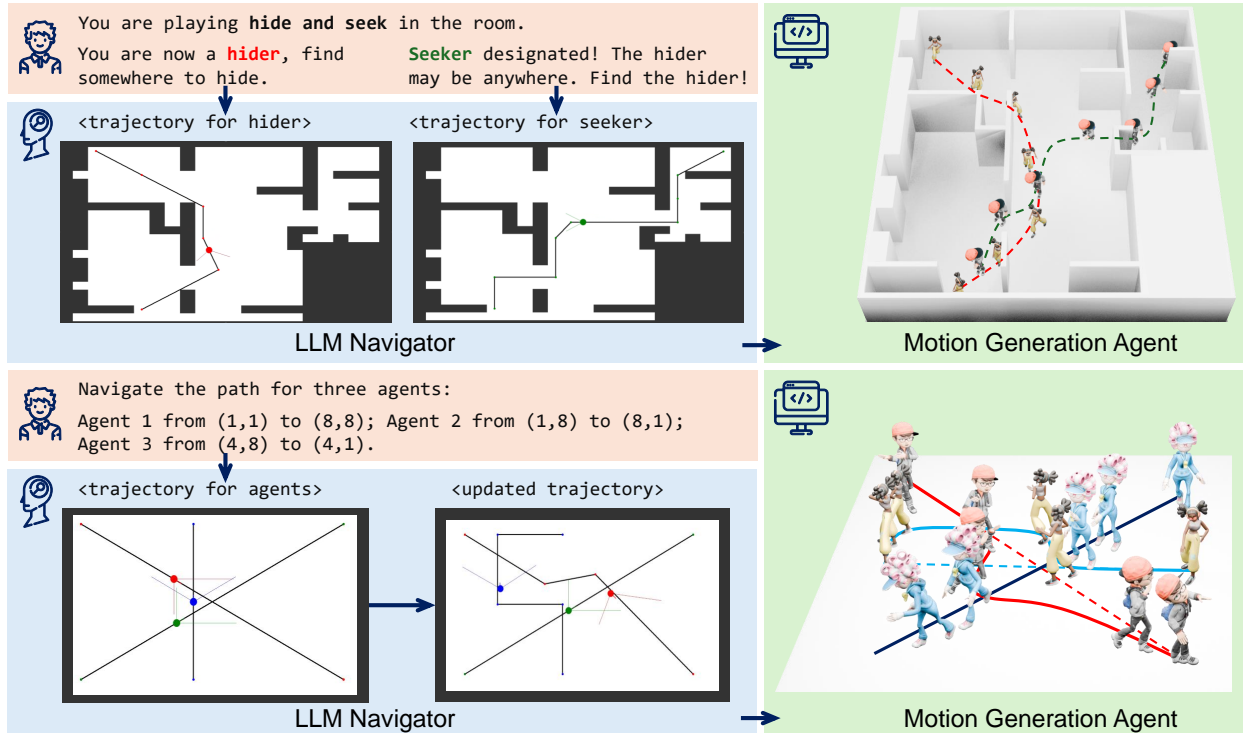


Figure 1. **Single agent** (top) navigating a real floor plan in a hide-and-seek scenario. **Multiple agents** (bottom) simultaneously move toward their destinations, the LLM autonomously resolves potential collisions. Our LLM-based system serves as an autonomous path navigator with zero-shot spatial reasoning capabilities, effectively handling obstacle avoidance and collision resolution in dynamic environments.

Abstract

Large Language Models (LLMs) have demonstrated strong generalizable reasoning and planning capabilities. However, their efficacies in spatial path planning and obstacle-free trajectory generation remain underexplored. Leveraging LLMs for navigation holds significant potential, given LLMs' ability to handle unseen scenarios, support user-agent interactions, and provide global control across complex systems, making them well-suited for agentic planning and humanoid motion generation. As one of the first studies in this domain, we explore the zero-shot navigation and path generation capabilities of LLMs by constructing a dataset and proposing an evaluation protocol. Specifically, we represent paths using anchor points con-

nected by straight lines, enabling movement in various directions. This approach offers greater flexibility and practicality compared to previous methods while remaining simple and intuitive for LLMs. We demonstrate that, when tasks are well-structured in this manner, modern LLMs exhibit substantial planning proficiency in avoiding obstacles while autonomously refining navigation with the generated motion to reach the target. Further, this spatial reasoning ability of a single LLM motion agent interacting in a static environment can be seamlessly generalized in multi-motion agents coordination in dynamic environments. Unlike traditional approaches that rely on single-step planning or local policies, our training-free LLM-based method enables global, dynamic, closed-loop planning, and autonomously resolving collision issues.

*Equal contribution.

1. Introduction

Large Language Models (LLMs) [1, 8, 34, 35] have made significant strides in reasoning and planning across various domains. These models exhibit powerful generalization capabilities, enabling them to handle unseen scenarios with remarkable flexibility and comprehension of world knowledge [11, 29, 31, 32, 40, 42, 43]. Despite their successes, the application of LLMs to spatial pathfinding and obstacle-free trajectory generation has received limited attention, particularly in real-world settings.

Recent work has explored the spatial reasoning abilities of LLMs [3, 19, 42, 45, 46, 49], but much of this research has focused on synthetic environments, with performance still falling short for real-world applicability. In contrast, deep reinforcement learning (RL)-based methods such as [18, 39, 55] have demonstrated substantial progress in autonomous navigation and pathfinding tasks. However, these approaches often require extensive training, involving large amounts of data and repeated interactions with the environment, making them impractical or costly when data collection is time-consuming or expensive. Additionally, RL methods struggle with handling unseen or unmodeled cases, a challenge where LLMs hold significant promise.

In this work, we explore the potential of pretrained LLMs for zero-shot path navigation in diverse environments, focusing on real-world applications like humanoid motion synthesis. Our approach with LLMs facilitates intuitive user-agent interactions, which enhances task completion and refinement, making them well-suited for applications in agent-based planning, humanoid motion generation, and multi-agent coordination. To make navigation tasks amenable to LLMs, we represent the environment (e.g., floor maps), agents, and paths as tokens that interact within a shared space. This token-based representation enables efficient spatial reasoning, providing robust and flexible solutions for pathfinding in complex environments. Specifically, we represent paths as sequences of sparse anchor points, allowing agents to move flexibly to any position within the space, rather than relying on predefined movement sets (e.g., 4 or 8 adjacent positions), as seen in previous works [2, 3, 19, 42, 47]. This approach aligns more closely with human intuition for maneuvering and obstacle avoidance, while also reducing the processing burden on the LLM.

We demonstrate the capabilities of our LLM-powered, training-free system through experiments on realistic floor-plans, evaluating the navigation abilities of various modern LLMs in both single-agent and multi-agent settings. Our results show that this approach generalizes effectively to previously unseen environments and tasks. Additionally, we showcase the system's ability to solve dynamic problems in closed-loop environments, where agent communication and coordination are essential to ensure robust navigation and

motion. Agents can autonomously adjust their plans and avoid collisions in real-time, highlighting the system's ability to handle complex, unpredictable scenarios. Finally, we highlight the potential of this system for humanoid motion generation, demonstrating how the system can generate realistic and contextually appropriate movements for agents in a wide range of dynamic environments. This work paves the way for real-world applications in areas such as autonomous robotics, virtual reality, and interactive human-robot interaction, where agents must navigate and collaborate in complex, dynamic spaces.

2. Related Work

2.1. Spatial Understanding and Reasoning

Effective navigation and planning in space require a fundamental understanding of the environment, a critical cognitive ability for both humans and intelligent systems. With the advancement of LLMs, spatial reasoning has become an emerging research focus. Studies such as [21–23, 41] investigate LLMs' spatial reasoning capabilities through verbal reasoning tasks, such as question answering (QA). Other works like [20] explore LLMs' ability to recognize patterns, while [12] focuses on enhancing LLMs' 3D reasoning capabilities. Additionally, [42] evaluates LLMs' performance in solving QA-based tiling puzzles. This paper aims to further explore and evaluate the capabilities of modern LLMs in standardized, structured, and realistic agent navigation tasks, demonstrating their effectiveness in understanding spatial environments and generating feasible solutions. Moreover, we showcase their downstream applications such as humanoid motion, extending beyond theoretical or virtual scenarios to more practical settings.

2.2. Using LLMs for Navigation

Recent LLM studies on path navigation apply to restricted scenarios. For example, [42] proposes a protocol to evaluate LLMs' ability to navigate in simple environments with a single possible route; [2, 3] investigate LLMs' pathfinding capabilities in square grids with simplified, synthetic environments; [19] explores using LLMs to navigate a single agent in a 5x5 grid without obstacles. All these studies focus on navigation within unreal environments with movements restricted to four directions (up, down, left, right), limiting their real-world applicability. Other works [17, 47, 50, 51, 54] employ language models for individual navigation tasks with camera inputs. In contrast, this paper addresses real-world challenges by enabling global planning for one or more agents, allowing navigation in realistic floor plans, while supporting dynamic collision resolution, further bridging the gap between simulation and real-world scenarios.

2.3. Environment-Aware Agents

Planning and controlling agents within environments is an area of increasing interest, with numerous real-world applications. This task typically involves obstacle-avoiding navigation and agent-environment interaction. Previous works have employed methods such as manually specified paths [52], the A* algorithm [9, 53], and diffusion models [48] to generate navigational paths. While these approaches perform well in static environments, they encounter limitations in more complex scenarios, particularly when multiple agents coexist. Multi-agent systems, in contrast to single-agent systems, introduce significantly greater complexity and remain relatively underexplored in continuous spaces [5, 14, 28, 30]. Some studies [15, 27] have used diffusion models to generate trajectories for multiple agents, but they do not address the challenges inherent in agent interaction. Conventionally, reinforcement learning (RL)-based methods [6, 10, 25, 53] have been utilized to produce physically plausible movements in dynamic environments. However, these approaches often struggle with generalization across diverse scenarios. In this paper, we present a training-free, LLM-powered method that leverages the world knowledge and interactive capabilities of LLMs. Our approach facilitates agent planning and navigation in dynamic environments with multiple coexisting agents in a simple yet intuitive manner, enabling interactive communication in a way that mirrors how humans navigate and interact in complex, dynamic environments.

3. Dynamic Path Planning with LLMs

To make LLMs comprehend this task, we uniformly encode agents with their anchored trajectories and the environment as discrete text tokens interacting with each other as follows:

3.1. Agents with Anchored Trajectories

Echoing how humans navigate through their environment, we are not restricted to only a few discrete directions.

Instead, human paths resemble a sequence of anchor points connected by almost straight lines to avoid obstacles while minimizing the total travel distance. For instance, when someone moves from one room to another, they may first walk directly toward the door, then proceed straight to the door of the next room, and finally enter the target room. This anchor-based approach is intuitive for humans and can be easily adapted for LLM planning. In this framework, a path or trajectory is not necessarily dense; it only requires a sequence of key points, akin to decomposing a complex task into simpler sub-goals, which is well-suited for modern LLMs [26, 29, 31, 37, 38, 40, 43].

Formally, let \mathcal{X} denote the movable space of the agent, where each point $x \in \mathcal{X}$ represents a possible state of the

agent. A trajectory \mathcal{T} is defined as a sequence of points:

$$\mathcal{T} = \{x_1, x_2, \dots, x_k\},$$

where each point $x_i \in \mathcal{X}$ represents a position in the environment, and k is the number of anchor points in the path. The trajectory is generated by connecting these points with straight lines, and the travel distance can be formulated as:

$$D(\mathcal{T}) = \sum_{i=1}^{k-1} \|x_i - x_{i+1}\|_2,$$

where $\|\cdot\|_2$ denotes the Euclidean distance between two consecutive points. The task of path planning is to determine an optimal sequence of anchor points that connect the initial and goal states, while satisfying any environmental constraints.

A critical aspect of path planning is ensuring that the trajectory avoids obstacles, static or dynamic. Specifically, a sub-path between two consecutive anchor points x_i and x_{i+1} is valid if and only if there are no obstacles along the line segment connecting them. Formally, for each consecutive pair of points (x_i, x_{i+1}) , the sub-path is valid if:

$$\begin{aligned} \forall t \in [0, 1], \text{ such that } \gamma(t) = (1-t)x_i + tx_{i+1}, \\ \text{there exists no obstacle such that } \gamma(t) \in \mathcal{O}, \end{aligned}$$

where $\gamma(t)$ represents the linear interpolation between x_i and x_{i+1} , and \mathcal{O} denotes the set of obstacles in the environment. If this condition is satisfied for all consecutive pairs (x_i, x_{i+1}) , the trajectory \mathcal{T} is considered valid.

Thus, the path planning problem can be viewed as finding an optimal sequence of anchor points $\{x_1, x_2, \dots, x_k\}$ that minimize the total travel distance $D(\mathcal{T})$, while ensuring the trajectory avoids obstacles and adheres to other environmental constraints.

In multi-agent scenarios, the complexity of path planning increases, as the trajectories of different agents may intersect. While some intersections may be unavoidable or difficult to resolve, it is important to note that different agents occupy the same space at different times. Therefore, the actual trajectory of each agent can only be fully determined during testing, when the agents' interactions and timing can be accounted for in the dynamic environment.

3.2. Spatial Environment Representation

Among various alternatives, the most commonly used and intuitive representation of space is in the form of grids [3, 42, 47]. In this representation, the environment is discretized into a grid structure where each cell corresponds to a specific location, allowing for clear and precise definitions of free spaces, obstacles, and agent positions.

Alternatively, space can be represented using code-based descriptions [3], which can be more interpretable for LLMs.

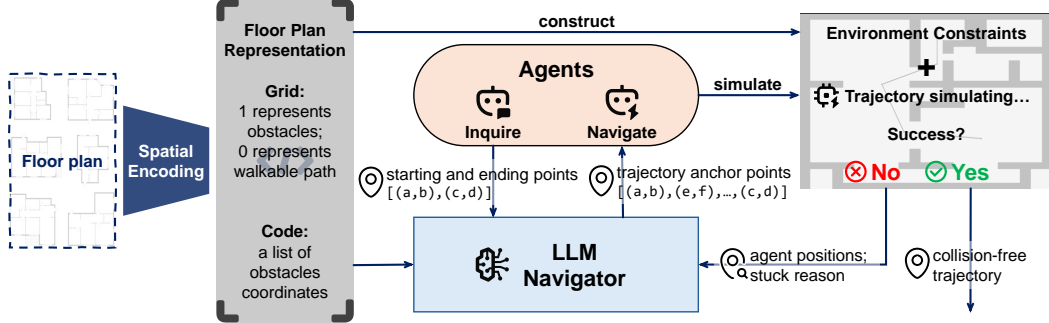


Figure 2. **Pipeline of our experiments.** The process begins with the input of a floor plan, followed by spatial encoding, agent navigation, and simulation. The LLM navigator generates the agent’s path, which is then validated and refined. If agents become stuck, they communicate with the LLM to resolve navigation issues.

This approach is both compact and flexible, enabling precise definitions of the environment through code. For instance, variables can be defined to specify the start and goal locations, while logic can be applied to place obstacles on the grid, shaping the environment accordingly. Intuitively, code provides a clear and concise way to define the task setting, making it a powerful alternative to traditional grid-based representations.

By using text-based representations, we bridge the gap between spatial reasoning and natural language processing, enabling LLMs to leverage their reasoning capabilities in a domain where they have proven effectiveness. This text-based approach sets ourselves apart from images as input, which may introduce unnecessary or redundant information such as textures, colors, or irrelevant details, while enabling the language capabilities of LLMs, which excel at processing and reasoning with text. To formalize, we define a grid-based environment representation:

$$\mathcal{G} = \{g_{i,j} \mid g_{i,j} \in \{0, 1\}\}$$

where $g_{i,j} = 1$ indicates an obstacle, $g_{i,j} = 0$ denotes free space, and $g_{i,j}$ represents the cell at row i and column j in a 2D grid.

We also define a code representation as a list of obstacle coordinates:

$$\mathcal{C} = \text{obstacles.append}((i_1, j_1), \dots, (i_n, j_n))$$

where each (i_k, j_k) denotes the location of an obstacle.

3.3. System Architecture

3.3.1. Overview

The architecture of the LLM-centered system is shown in Figure 2. Let the floor map be firstly encoded into a grid-based \mathcal{G} or code-based \mathcal{C} format. This encoded floorplan constructs an environment \mathcal{E} , and is passed to the LLM \mathcal{L} .

Given N agents, each agent i has a starting point s_i and a target point t_i . The LLM generates the trajectories \mathcal{T}_i for all

agents based on the starting points $S = \{s_i\}_{i=1}^N$ and target points $T = \{t_i\}_{i=1}^N$:

$$\mathcal{T} = \mathcal{L}(\mathcal{E}, S, T) = \{x_1^{(i)}, x_2^{(i)}, \dots, x_{k_i}^{(i)}\}_{i=1}^N$$

The agents are simulated in the environment \mathcal{E} . If a collision occurs at time t , the agent queries the LLM using its current position $\mathbf{p}_i(t)$ and the set of detected collisions \mathcal{C}_t , requesting a refined path \mathcal{T}'_i .

The final output consists of the collision-free trajectories \mathcal{T}'_i for all agents, ensuring that each agent reaches its target point without collisions.

3.3.2. Path Refining Strategies

To handle collisions with static obstacles (floorplan) or dynamic obstacles (motion agents), we capitalize LLMs’ multi-turn capability, allowing for iterative refinement outputs until achieving the desired result. We propose two transformative update strategies to refine the path: (1) *additive* and (2) *compositional*, drawing inspiration from image alignment warping source to target [4]. The additive approach recalculates the entire motion plan holistically, integrating all prior adjustments into a unified transformation—similar to continuously recalculating an optimal golf swing based on previous strokes. While straightforward, this method can be inefficient, as each update effectively resets to the origin. In contrast, the compositional approach refines the trajectory incrementally, making step-by-step corrections based on the current state. Though generally more efficient, it may suffer if an update places the trajectory in an unfavorable position (e.g., low terrain where the ball becomes stuck), potentially hindering future corrections.

In our setting, let s denote the starting point and t the destination. Given n update opportunities, if an agent becomes stuck during the i -th trial for a reason r (which includes its current stuck position), the *additive* strategy updates the trajectory as

$$\mathcal{T}_{i+1} = \mathcal{L}(s, t, r),$$

implying that each update is computed globally, restarting from the original starting point s .

In contrast, the *compositional* strategy refines the trajectory based on the current state. Let p_i denote the current stopping position at iteration i when the path is unsuccessful. Then, the updated trajectory is computed as

$$\mathcal{T}_{i+1} = \mathcal{L}(p_i, t, r),$$

indicating that the current stuck position serves as the new starting point for planning the remainder of the path. Each corrective adjustment is applied "on-the-fly" to the current trajectory, enabling dynamic, incremental updates.

When multiple agents become stuck simultaneously, the LLM can coordinate across them using either strategy to refine their paths.

4. Experiments

4.1. Experiment Setup

4.1.1. Dataset

To ensure the applicability of our problem to real-world scenarios while maintaining simplicity, we build on the R2V dataset [16], which contains 815 realistic floorplans from actual buildings. The floor plans are primarily rectilinear in shape, making them easier for LLMs to process and understand.

For each floor plan, we first convert it into textual formats and randomly sample three pairs of starting and target points. We then use the A* algorithm to generate obstacle-free optimal paths as ground truth labels, creating a dataset suitable for evaluating the spatial navigation ability of LLMs. In addition to this dataset, we have also manually created more complex scenarios to explore the upper bound of LLMs' navigation and planning capabilities, inspiring broader exploration in this domain.

4.1.2. Evaluation Metrics

To evaluate the performance of LLMs, we use several standard metrics: Success Rate (SR), Success weighted by Path Length (SPL), Completion Rate (CR), and Weighted Success Rate (WSR). These metrics are commonly used in navigation and path planning tasks to assess both the efficiency and effectiveness of the trajectory generation.

- **Success Rate (SR):** The success rate is defined as the percentage of test cases where the agent successfully reaches the goal:

$$SR = \frac{1}{N} \sum_{i=1}^N \mathbb{I}(\text{success}_i),$$

where $\mathbb{I}(\text{success}_i)$ is an indicator function that returns 1 if the agent successfully reaches the target and 0 otherwise, and N is the total number of test cases.

- **Success weighted by Path Length (SPL):** SPL accounts for both the success rate and the efficiency of the path:

$$SPL = \frac{1}{N} \sum_{i=1}^N \frac{\mathbb{I}(\text{success}_i) \cdot d_i}{\max(d_i, d_{\text{opt},i})},$$

where d_i is the length of the trajectory taken by the agent, and $d_{\text{opt},i}$ is the optimal path length for the i -th test case. The SPL metric rewards shorter, more efficient paths while penalizing longer, inefficient paths.

- **Completion Rate (CR):** The completion rate measures the fraction of the total path length that the agent is able to complete. It is defined as:

$$CR = \frac{1}{N} \sum_{i=1}^N \frac{d_i}{d_{\text{total},i}},$$

where d_i is the length of the trajectory taken by the agent, and $d_{\text{total},i}$ is the total length of the path the agent was supposed to cover in the i -th test case. The CR metric emphasizes how much of the planned path is successfully completed, regardless of success or failure.

- **Weighted Success Rate (WSR):** WSR is a metric that assigns higher weights to longer paths, reflecting their cost or complexity, defined as:

$$WSR = \frac{1}{\sum_{i=1}^N d_{\text{opt},i}} \sum_{i=1}^N \mathbb{I}(\text{success}_i) \cdot d_{\text{opt},i},$$

where $d_{\text{opt},i}$ is the length of the optimal path, which can also reflect the difficulty of the test case. The denominator normalizes the WSR across all test cases, ensuring that the sum of WSR equals 1 by considering the total optimal path length.

These metrics provide a comprehensive evaluation of LLMs' navigation performance by accounting for both the success rate and efficiency of the generated trajectories, as

Models	Type	Input	SR \uparrow	SPL \uparrow	CR \uparrow	WSR \uparrow
<i>Baseline</i>	-	-	0.370	0.370	0.370	0.207
Claude-3.5-Sonnet	general	code	0.453	0.437	0.556	0.307
		grid	0.330	0.302	0.426	0.183
Llama-3.3-70B	general	code	0.397	0.316	0.565	0.240
		grid	0.350	0.296	0.520	0.197
Gemini-2.0-flash	general	code	0.380	0.297	0.541	0.205
		grid	0.273	0.223	0.328	0.139
GPT-4o	multimodal	code	0.420	0.381	0.560	0.291
		grid	0.387	0.376	0.477	0.227
		image	0.370	0.349	0.477	0.222
DeepSeek-R1	reasoning	code	0.673	0.645	0.766	0.520
		grid	0.650	0.623	0.729	0.503
o3-mini	reasoning	code	0.507	0.488	0.590	0.396
		grid	0.781	0.710	0.828	0.665

Table 1. Zero-shot path navigation performance of various LLMs for single-agent scenarios in a single trial.

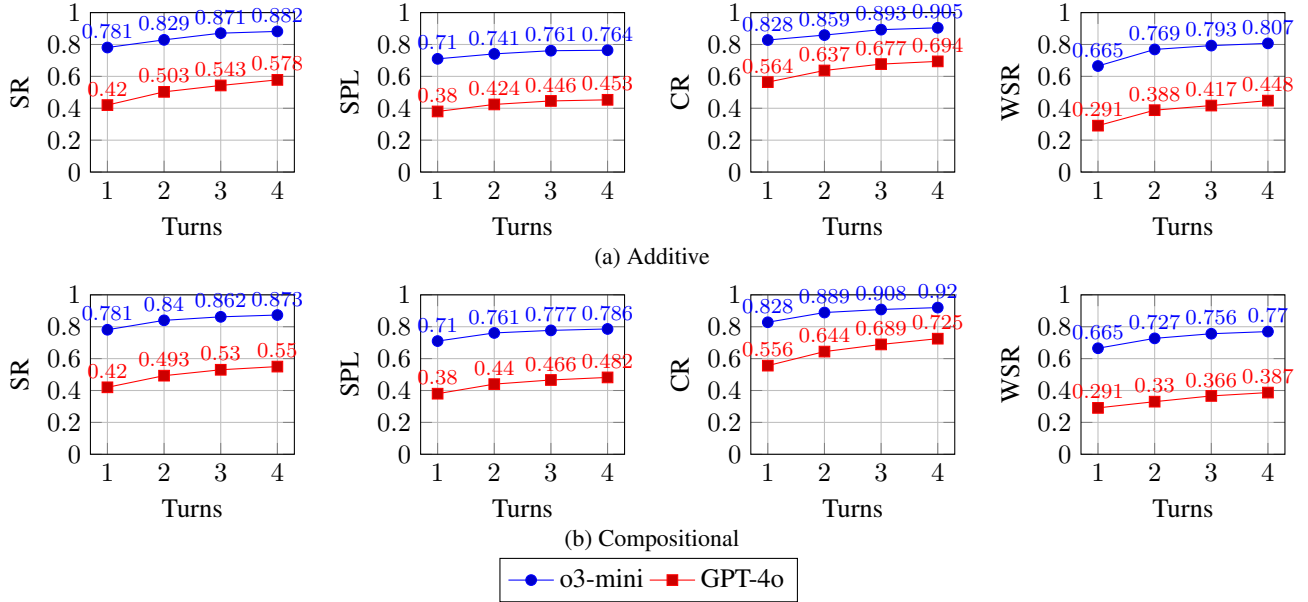


Figure 3. Additive and compositional strategies for multi-turn navigation refining.

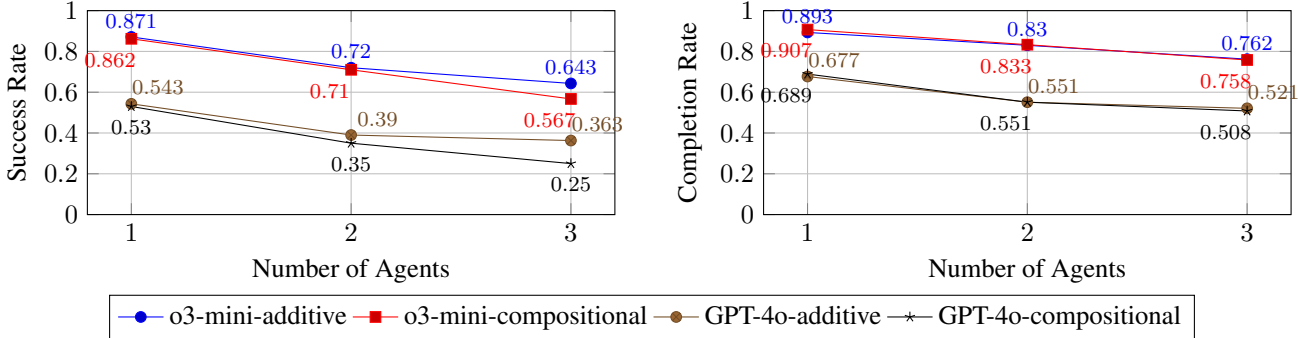


Figure 4. Success Rate (SR) and Completing Rate (CR) for different numbers of agents.

well as task completion and complexity. Combined with our constructed dataset, we propose a protocol to benchmark the spatial navigation capabilities of LLMs.

4.2. Quantitative Results

We evaluate a range of LLMs, including GPT-4o [13], Gemini [33], DeepSeek [8], Llama [7], OpenAI o3-mini, and Claude-Sonnet. Our selection comprises both state-of-the-art reasoning models and prior general-purpose models. We conduct extensive experiments, including benchmarking and ablation studies. All of our experiments are in a *zero-shot* setting.

4.2.1. Single-Agent

First, we assess how LLMs perform in a single attempt. As a baseline, we use scores obtained by moving directly from the starting point to the destination without any navigation. For input, we examine both grid and code representations, as described above. Additionally, we explore direct image input without spatial encoding, where the start and

end points are marked on the image.

The results, presented in Table 1, indicate that modern models with advanced reasoning capabilities demonstrate significantly stronger performance in spatial navigation tasks. Furthermore, textual input outperforms image-based input, highlighting the effectiveness of textual representations, which align more naturally with LLMs' ability to process structured, discrete text-based information. When comparing the two textual formats, their effectiveness varies across models. For most models, code-based input yields better performance, as it explicitly encodes coordinates. However, for o3-mini, which exhibits strong reasoning capabilities, the grid-based format proves more effective. We attribute this to its ability to intuitively recognize spatial patterns, akin to human interpretation.

We also investigate how the LLM-based system benefits from multi-turn interactions. We evaluate and compare the *additive* and *compositional* approaches, with results shown in Figure 3. As the number of turns increases,

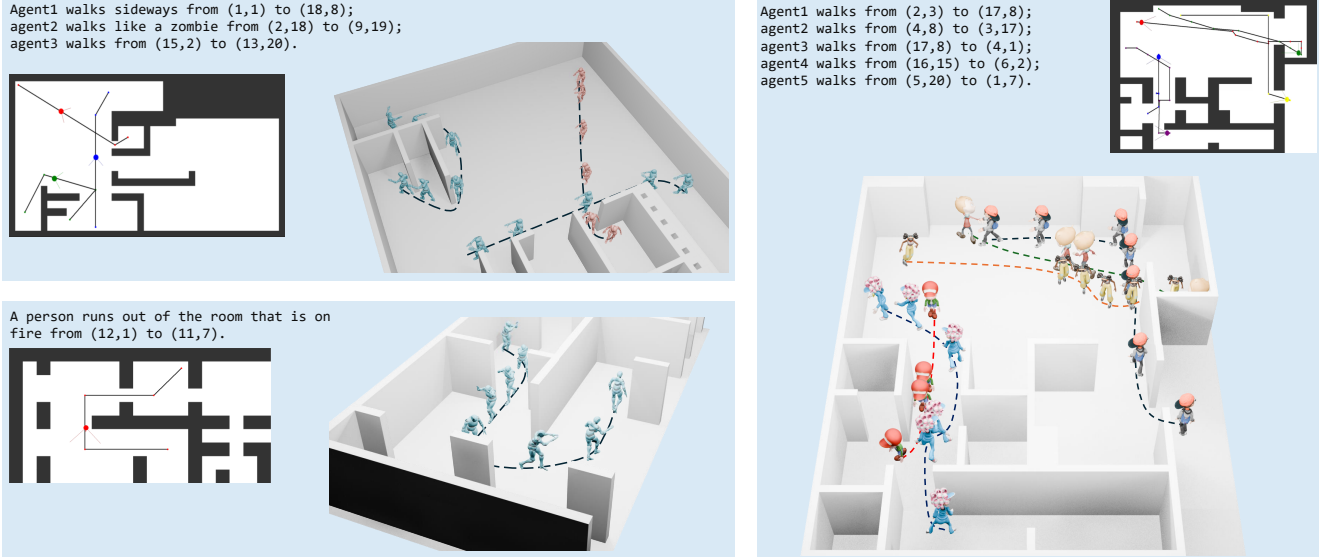


Figure 5. Top-down views of the generated final trajectory and visualized humanoid motion results. Agents successfully navigate to their intended destinations while avoiding obstacles and other agents.

both methods contribute to overall performance improvement. The *additive* approach generally achieves a higher success rate (both SR and WSR), as it recalculates the complete path from the origin at each step. In contrast, the *compositional* approach, while more susceptible to suboptimal adjustments—analogous to a poor stroke in golf affecting subsequent corrections—exhibits higher SPL and CR, as it refines the current trajectory without resetting, preserving progress and ensuring continuous improvement.

4.2.2. Multi-Agents

We extend our experiments to scenarios with two and three agents, with the results shown in Figure 4. In these experiments, the maximum number of retries is set to three. This setup introduces additional complexity, as each agent must navigate to its destination while avoiding obstacles and dynamically resolve collisions with other agents, making the system more interactive and adaptive.

Our results indicate that as the number of agents increases, the performance scores decrease, but they remain within a reasonable and practical range. This demonstrates the feasibility of multi-agent coordination and LLMs’ ability to manage complex, dynamic environments. Additionally, different update strategies show minimal impact on overall performance. The *compositional* approach tends to yield slightly lower scores, which aligns with real-world observations—for instance, when two people walk toward each other and both instinctively step in the same direction to avoid a collision, they may inadvertently create an awkward situation. This suggests that the *additive* approach may be more effective in globally resolving such coordination conflicts.

Overall, modern LLMs, such as o3-mini, demonstrate substantial capabilities in spatial navigation tasks, achieving approximately 80% SR in a single trial and up to about 90% SR with multiple trials for single-agent scenarios. The system can also be seamlessly extended to multi-agent scenarios without much performance degradation. Moreover, all experiments are conducted in a zero-shot setting, further validating LLMs’ reasoning abilities and world knowledge. Taken together, these results indicate that modern LLMs are becoming increasingly applicable to real-world agent scenarios.

4.3. Qualitative Results

In this section, we visualize our results and introduce a practical application involving generating environment-aware humanoid motion (Figure 6). Previous works, such as OmniControl [44] and TLControl [36], support trajectory control; however, they rely on *manually* defined input trajectories.

Frameworks like Motion-Agent [40] leverages LLMs to automatically decompose complex user requests and generate motion through a motion generation agent, enabling natural user-agent interaction. By integrating these approaches, we demonstrate that our LLM-based navigation system can be seamlessly applied to humanoid motion as a downstream task. Furthermore, our approach can be readily extended to scenarios involving multiple agents coexisting within an environment. This application method is illustrated in Figure 6. Once the system generates an obstacle-free trajectory, it can be used to guide motion generation models — which are inherently non-environment-aware —

to follow the trajectory and thus avoid collisions.

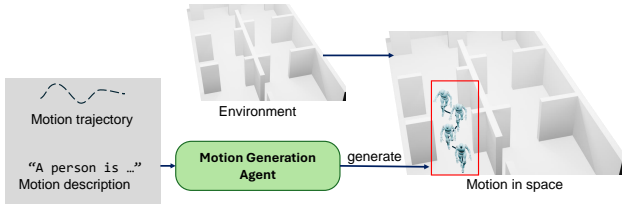


Figure 6. When paired with motion generation agents, the system can generate environment-aware, realistic motions.

We provide both the top-down view and 3D humanoid motions in Figure 5, demonstrating that our LLM-based system can navigate effectively for both single and multiple agents. While the initially generated path may sometimes be infeasible, the system can autonomously adjust itself multiple times to resolve such issues. Notably, in the example on the right, where five agents encounter different challenges, the system successfully coordinates their paths through multiple adjustments, enabling them to avoid obstacles and one another, ultimately reaching their respective destinations.

Furthermore, we extend the input floor map to 3D (or more precisely, 2.5D), where instead of using 1 and 0 to represent obstacles and free space, each point is assigned a height value, forming a height map. Consequently, the output path is represented using anchor points in three dimensions. As shown in Figure 7, this extension enables our system to generate agent paths that are not restricted to a flat plane. Additionally, our system has the potential to be integrated with methods like SCENIC [52], which can interact with the scene but rely on manually defined input trajectories to avoid obstacles.

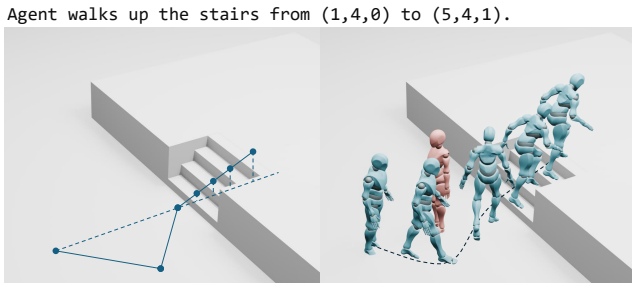


Figure 7. The system generates a 3D path and guides the blue agent to move within the 3D space while avoiding the red agent intruding during execution, by adjusting the path.

5. Discussion

RL-agents vs LLM-agents. While modern LLMs are not at odds with RL as they are trained with RLHF [1, 24],

in stark contrast to conventional deep RL in robot path planning which stresses on optimizing expected discounted return (for single-agent RL) and the equilibrium of joint policies (in multi-agent RL), typically with considerable amount of training data, this paper demonstrates the zero-shot, training-free ability across modern LLMs in path planning and dynamic navigation in single-agent and multi-agent scenarios, evaluated on completion rate, success rate and path length which, albeit their simplicity and lack of sophistication compared to the specific and formal RL optimization objectives, are arguably equally relevant to any autonomous systems in evaluating their performance.

Limitations and Future Work. Our first work on LLM-navigation focuses on dynamic systems, including multi-agent scenarios, and has been validated using a simulated environment. Although these simulations offer valuable insights into system effectiveness, the lack of real-world testing—particularly with physical robots and in household scenarios—necessitates further validation in dynamic, real-world settings. Additionally, our current approach relies on a globally encoded floorplan that assumes full observability during path planning. In many robotic applications, however, only partial observations of the environment are available during navigation. Future work will explore replacing the global floorplan embedding with a local embedding strategy that focuses on the immediate surroundings observable by each agent at the current timestamp. Nevertheless, our framework is inherently generalizable, capable of seamlessly incorporating additional functionalities such as collision handling and agent-agent interactions, which can be managed as local operations.

Concluding Remarks. In this work, we examined the reasoning capabilities of large language models (LLMs) in spatial navigation and collision-free trajectory generation for motion agents in dynamic environments. We represent floor maps as discrete text and structure navigation paths using a sparse anchored representation. As one of the first studies on LLMs’ spatial reasoning, we constructed a comprehensive dataset and proposed evaluation protocols to assess their performance. Furthermore, we extended our investigation to scenarios involving multiple coexisting agents. Our results demonstrate that LLMs can effectively coordinate across agents and autonomously resolve collisions in closed-loop, dynamic settings. We also showcased the real-world applicability of our approach by applying it to the task of humanoid motion. Overall, our work advances the development of intelligent systems that better perceive and understand the real world, make appropriate decisions, and enable interactive engagement with users and other agents, thereby paving the way for real-world applications.

References

[1] Josh Achiam, Steven Adler, Sandhini Agarwal, Lama Ahmad, Ilge Akkaya, Florencia Leoni Aleman, Diogo Almeida, Janko Altenschmidt, Sam Altman, Shyamal Anadkat, et al. Gpt-4 technical report. *arXiv preprint arXiv:2303.08774*, 2023. 2, 8

[2] Mohamed Aghzal, Erion Plaku, and Ziyu Yao. Can large language models be good path planners? a benchmark and investigation on spatial-temporal reasoning. *arXiv preprint arXiv:2310.03249*, 2023. 2

[3] Mohamed Aghzal, Erion Plaku, and Ziyu Yao. Look further ahead: Testing the limits of gpt-4 in path planning. In *2024 IEEE 20th International Conference on Automation Science and Engineering (CASE)*, pages 1020–1027. IEEE, 2024. 2, 3

[4] Simon Baker and Iain Matthews. Lucas-kanade 20 years on: A unifying framework. *International journal of computer vision*, 56:221–255, 2004. 4

[5] Joao Carvalho, An T Le, Mark Baierl, Dorothea Koert, and Jan Peters. Motion planning diffusion: Learning and planning of robot motions with diffusion models. In *2023 IEEE/RSJ International Conference on Intelligent Robots and Systems (IROS)*, pages 1916–1923. IEEE, 2023. 3

[6] Yu-Wei Chao, Jimei Yang, Weifeng Chen, and Jia Deng. Learning to sit: Synthesizing human-chair interactions via hierarchical control. In *Proceedings of the AAAI Conference on Artificial Intelligence*, pages 5887–5895, 2021. 3

[7] Abhimanyu Dubey, Abhinav Jauhri, Abhinav Pandey, Abhishek Kadian, Ahmad Al-Dahle, Aiesha Letman, Akhil Mathur, Alan Schelten, Amy Yang, Angela Fan, et al. The llama 3 herd of models. *arXiv preprint arXiv:2407.21783*, 2024. 6

[8] Daya Guo, Dejian Yang, Haowei Zhang, Junxiao Song, Ruoyu Zhang, Runxin Xu, Qihao Zhu, Shirong Ma, Peiyi Wang, Xiao Bi, et al. Deepseek-r1: Incentivizing reasoning capability in llms via reinforcement learning. *arXiv preprint arXiv:2501.12948*, 2025. 2, 6

[9] Mohamed Hassan, Duygu Ceylan, Ruben Villegas, Jun Saito, Jimei Yang, Yi Zhou, and Michael Black. Stochastic scene-aware motion prediction. In *Proceedings of the International Conference on Computer Vision 2021*, 2021. 3

[10] Mohamed Hassan, Yunrong Guo, Tingwu Wang, Michael Black, Sanja Fidler, and Xue Bin Peng. Synthesizing physical character-scene interactions. In *ACM SIGGRAPH 2023 Conference Proceedings*, pages 1–9, 2023. 3

[11] Dan Hendrycks, Collin Burns, Saurav Kadavath, Akul Arora, Steven Basart, Eric Tang, Dawn Song, and Jacob Steinhardt. Measuring mathematical problem solving with the math dataset. *arXiv preprint arXiv:2103.03874*, 2021. 2

[12] Yining Hong, Haoyu Zhen, Peihao Chen, Shuhong Zheng, Yilun Du, Zhenfang Chen, and Chuang Gan. 3d-llm: Injecting the 3d world into large language models. *Advances in Neural Information Processing Systems*, 36:20482–20494, 2023. 2

[13] Aaron Hurst, Adam Lerer, Adam P Goucher, Adam Perelman, Aditya Ramesh, Aidan Clark, AJ Ostrow, Akila Welinda, Alan Hayes, Alec Radford, et al. Gpt-4o system card. *arXiv preprint arXiv:2410.21276*, 2024. 6

[14] Jiaoyang Li, Andrew Tinka, Scott Kiesel, Joseph W Durham, TK Satish Kumar, and Sven Koenig. Lifelong multi-agent path finding in large-scale warehouses. In *Proceedings of the AAAI Conference on Artificial Intelligence*, pages 11272–11281, 2021. 3

[15] Jinhao Liang, Jacob K Christopher, Sven Koenig, and Ferdinando Fioretto. Multi-agent path finding in continuous spaces with projected diffusion models. *arXiv preprint arXiv:2412.17993*, 2024. 3

[16] Chen Liu, Jiajun Wu, Pushmeet Kohli, and Yasutaka Furukawa. Raster-to-vector: Revisiting floorplan transformation. In *Proceedings of the IEEE International Conference on Computer Vision*, pages 2195–2203, 2017. 5

[17] Yuecheng Liu, Dafeng Chi, Shiguang Wu, Zhanguang Zhang, Yaochen Hu, Lingfeng Zhang, Yingxue Zhang, Shuang Wu, Tongtong Cao, Guowei Huang, et al. Spatialcot: Advancing spatial reasoning through coordinate alignment and chain-of-thought for embodied task planning. *arXiv preprint arXiv:2501.10074*, 2025. 2

[18] Yunlian Lyu, Yimin Shi, and Xianggang Zhang. Improving target-driven visual navigation with attention on 3d spatial relationships. *Neural Processing Letters*, 54(5):3979–3998, 2022. 2

[19] Nicolas Martorell. From text to space: Mapping abstract spatial models in llms during a grid-world navigation task. *arXiv preprint arXiv:2502.16690*, 2025. 2

[20] Suvir Mirchandani, Fei Xia, Pete Florence, Brian Ichter, Danny Driess, Montserrat Gonzalez Arenas, Kanishka Rao, Dorsa Sadigh, and Andy Zeng. Large language models as general pattern machines. *arXiv preprint arXiv:2307.04721*, 2023. 2

[21] Roshanak Mirzaee and Parisa Kordjamshidi. Transfer learning with synthetic corpora for spatial role labeling and reasoning. *arXiv preprint arXiv:2210.16952*, 2022. 2

[22] Roshanak Mirzaee, Hossein Rajaby Faghihi, Qiang Ning, and Parisa Kordjamshidi. Spartqa: A textual question answering benchmark for spatial reasoning. *arXiv preprint arXiv:2104.05832*, 2021.

[23] Ida Momennejad, Hosein Hasanbeig, Felipe Vieira Frujeri, Hiteshi Sharma, Nebojsa Jojic, Hamid Palangi, Robert Ness, and Jonathan Larson. Evaluating cognitive maps and planning in large language models with cogeval. *Advances in Neural Information Processing Systems*, 36:69736–69751, 2023. 2

[24] Long Ouyang, Jeffrey Wu, Xu Jiang, Diogo Almeida, Carroll Wainwright, Pamela Mishkin, Chong Zhang, Sandhini Agarwal, Katarina Slama, Alex Ray, et al. Training language models to follow instructions with human feedback. *Advances in neural information processing systems*, 35:27730–27744, 2022. 8

[25] Xue Bin Peng, Yunrong Guo, Lina Halper, Sergey Levine, and Sanja Fidler. Ase: Large-scale reusable adversarial skill embeddings for physically simulated characters. *ACM Transactions On Graphics (TOG)*, 41(4):1–17, 2022. 3

[26] Archiki Prasad, Alexander Koller, Mareike Hartmann, Peter Clark, Ashish Sabharwal, Mohit Bansal, and Tushar Khot.

Adapt: As-needed decomposition and planning with language models. *arXiv preprint arXiv:2311.05772*, 2023. 3

[27] Davis Rempe, Zhengyi Luo, Xue Bin Peng, Ye Yuan, Kris Kitani, Karsten Kreis, Sanja Fidler, and Or Litany. Trace and pace: Controllable pedestrian animation via guided trajectory diffusion. In *Proceedings of the IEEE/CVF Conference on Computer Vision and Pattern Recognition*, pages 13756–13766, 2023. 3

[28] Yorai Shaoul, Itamar Mishani, Shivam Vats, Jiaoyang Li, and Maxim Likhachev. Multi-robot motion planning with diffusion models. *arXiv preprint arXiv:2410.03072*, 2024. 3

[29] Ishika Singh, Valts Blukis, Arsalan Mousavian, Ankit Goyal, Danfei Xu, Jonathan Tremblay, Dieter Fox, Jesse Thomason, and Animesh Garg. Progprompt: Generating situated robot task plans using large language models. In *2023 IEEE International Conference on Robotics and Automation (ICRA)*, pages 11523–11530. IEEE, 2023. 2, 3

[30] Roni Stern, Nathan Sturtevant, Ariel Felner, Sven Koenig, Hang Ma, Thayne Walker, Jiaoyang Li, Dor Atzman, Liron Cohen, TK Kumar, et al. Multi-agent pathfinding: Definitions, variants, and benchmarks. In *Proceedings of the International Symposium on Combinatorial Search*, pages 151–158, 2019. 3

[31] Haotian Sun, Yuchen Zhuang, Lingkai Kong, Bo Dai, and Chao Zhang. Adaplayer: Adaptive planning from feedback with language models. *Advances in neural information processing systems*, 36:58202–58245, 2023. 2, 3

[32] Shanlin Sun, Gabriel De Araujo, Jiaqi Xu, Shenghan Zhou, Hanwen Zhang, Ziheng Huang, Chenyu You, and Xiaohui Xie. Coma: Compositional human motion generation with multi-modal agents. *arXiv preprint arXiv:2412.07320*, 2024. 2

[33] Gemini Team, Rohan Anil, Sebastian Borgeaud, Jean-Baptiste Alayrac, Jiahui Yu, Radu Soricut, Johan Schalkwyk, Andrew M Dai, Anja Hauth, Katie Millican, et al. Gemini: a family of highly capable multimodal models. *arXiv preprint arXiv:2312.11805*, 2023. 6

[34] Gemma Team, Morgane Riviere, Shreya Pathak, Pier Giuseppe Sessa, Cassidy Hardin, Surya Bhupatiraju, Léonard Hussenot, Thomas Mesnard, Bobak Shahriari, Alexandre Ramé, et al. Gemma 2: Improving open language models at a practical size. *arXiv preprint arXiv:2408.00118*, 2024. 2

[35] Hugo Touvron, Thibaut Lavril, Gautier Izacard, Xavier Martinet, Marie-Anne Lachaux, Timothée Lacroix, Baptiste Rozière, Naman Goyal, Eric Hambro, Faisal Azhar, et al. Llama: Open and efficient foundation language models. *arXiv preprint arXiv:2302.13971*, 2023. 2

[36] Weilin Wan, Zhiyang Dou, Taku Komura, Wenping Wang, Dinesh Jayaraman, and Lingjie Liu. Tlcontrol: Trajectory and language control for human motion synthesis. In *European Conference on Computer Vision*, pages 37–54. Springer, 2024. 7

[37] Zihao Wang, Shaofei Cai, Guanzhou Chen, Anji Liu, Xiaojian Ma, and Yitao Liang. Describe, explain, plan and select: Interactive planning with large language models enables open-world multi-task agents. *arXiv preprint arXiv:2302.01560*, 2023. 3

[38] Zixuan Wang, Yu-Wing Tai, and Chi-Keung Tang. Audio-agent: Leveraging llms for audio generation, editing and composition. *arXiv preprint arXiv:2410.03335*, 2024. 3

[39] Erik Wijmans, Abhishek Kadian, Ari Morcos, Stefan Lee, Irfan Essa, Devi Parikh, Manolis Savva, and Dhruv Batra. Dd-ppo: Learning near-perfect pointgoal navigators from 2.5 billion frames. *arXiv preprint arXiv:1911.00357*, 2019. 2

[40] Qi Wu, Yubo Zhao, Yifan Wang, Xinhang Liu, Yu-Wing Tai, and Chi-Keung Tang. Motion-agent: A conversational framework for human motion generation with llms. *arXiv preprint arXiv:2405.17013*, 2024. 2, 3, 7

[41] Ruoling Wu and Danhuai Guo. Do large language models have spatial cognitive abilities? *ACM Transactions on Intelligent Systems and Technology*. 2

[42] Wenshan Wu, Shaoguang Mao, Yadong Zhang, Yan Xia, Li Dong, Lei Cui, and Furu Wei. Mind’s eye of llms: Visualization-of-thought elicits spatial reasoning in large language models. In *The Thirty-eighth Annual Conference on Neural Information Processing Systems*, 2024. 2, 3

[43] Xixi Wu, Yifei Shen, Caihua Shan, Kaitao Song, Siwei Wang, Bohang Zhang, Jiarui Feng, Hong Cheng, Wei Chen, Yun Xiong, et al. Can graph learning improve planning in llm-based agents? In *The Thirty-eighth Annual Conference on Neural Information Processing Systems*, 2024. 2, 3

[44] Yiming Xie, Varun Jampani, Lei Zhong, Deqing Sun, and Huaizu Jiang. Omnicontrol: Control any joint at any time for human motion generation. *arXiv preprint arXiv:2310.08580*, 2023. 7

[45] Liuchang Xu, Shuo Zhao, Qingming Lin, Luyao Chen, Qian-qian Luo, Sensen Wu, Xinyue Ye, Hailin Feng, and Zhen-hong Du. Evaluating large language models on spatial tasks: A multi-task benchmarking study. *arXiv preprint arXiv:2408.14438*, 2024. 2

[46] Yutaro Yamada, Yihan Bao, Andrew K Lampinen, Jungo Kasai, and Ilker Yildirim. Evaluating spatial understanding of large language models. *arXiv preprint arXiv:2310.14540*, 2023. 2

[47] Jihan Yang, Shusheng Yang, Anjali W Gupta, Rilyn Han, Li Fei-Fei, and Saining Xie. Thinking in space: How multimodal large language models see, remember, and recall spaces. *arXiv preprint arXiv:2412.14171*, 2024. 2, 3

[48] Hongwei Yi, Justus Thies, Michael J Black, Xue Bin Peng, and Davis Rempe. Generating human interaction motions in scenes with text control. In *European Conference on Computer Vision*, pages 246–263. Springer, 2024. 3

[49] Hang Yin, Zhifeng Lin, Xin Liu, Bin Sun, and Kan Li. Do multimodal language models really understand direction? a benchmark for compass direction reasoning. *arXiv preprint arXiv:2412.16599*, 2024. 2

[50] Bangguo Yu, Hamidreza Kasaei, and Ming Cao. L3mvn: Leveraging large language models for visual target navigation. In *2023 IEEE/RSJ International Conference on Intelligent Robots and Systems (IROS)*, pages 3554–3560. IEEE, 2023. 2

[51] Wentao Yuan, Jiafei Duan, Valts Blukis, Wilbert Pumacay, Ranjay Krishna, Adithyavairavan Murali, Arsalan Mousavian, and Dieter Fox. Robopoint: A vision-language model

for spatial affordance prediction for robotics. *arXiv preprint arXiv:2406.10721*, 2024. [2](#)

[52] Xiaohan Zhang, Sebastian Starke, Vladimir Guzov, Zhen-song Zhang, Eduardo Pérez Pellitero, and Gerard Pons-Moll. Scenic: Scene-aware semantic navigation with instruction-guided control. *arXiv preprint arXiv:2412.15664*, 2024. [3](#), [8](#)

[53] Kaifeng Zhao, Yan Zhang, Shaofei Wang, Thabo Beeler, and Siyu Tang. Synthesizing diverse human motions in 3d indoor scenes. In *Proceedings of the IEEE/CVF international conference on computer vision*, pages 14738–14749, 2023. [3](#)

[54] Kaiwen Zhou, Kaizhi Zheng, Connor Pryor, Yilin Shen, Hongxia Jin, Lise Getoor, and Xin Eric Wang. Esc: Exploration with soft commonsense constraints for zero-shot object navigation. In *International Conference on Machine Learning*, pages 42829–42842. PMLR, 2023. [2](#)

[55] Yuke Zhu, Roozbeh Mottaghi, Eric Kolve, Joseph J Lim, Abhinav Gupta, Li Fei-Fei, and Ali Farhadi. Target-driven visual navigation in indoor scenes using deep reinforcement learning. In *2017 IEEE international conference on robotics and automation (ICRA)*, pages 3357–3364. IEEE, 2017. [2](#)

Dynamic Path Navigation for Motion Agents with LLM Reasoning

Supplementary Material

A. More Qualitative Results

We provide additional qualitative results in the supplementary material, including attached videos and an HTML file for better visualization.

Here, we present some final generated trajectories in top-down views.

Figure 1 illustrates the capability of the LLM to effectively manage and resolve complex and challenging scenarios.

Figure 2 demonstrates how the additive strategy utilizes a restart mechanism to successfully avoid obstacles.

Figure 3 demonstrates how the compositional strategy effectively dynamically avoid obstacles “on the fly”.



Figure 1. More qualitative results in top-down view.



Figure 2. Additive Strategy

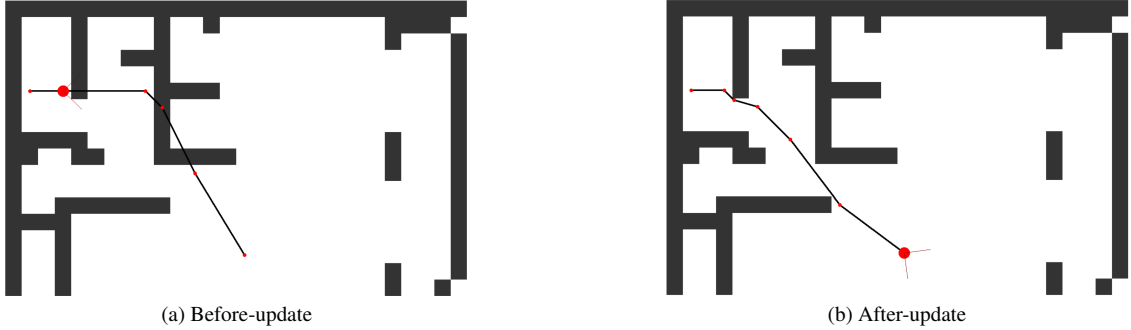


Figure 3. Compositional strategy

B. Dataset Processing

B.1. Spatial Encoding

Given an input floor plan image $I \in \mathbb{R}^{H \times W \times 3}$, we first convert it to a grayscale image:

$$I_g = \text{Grayscale}(I), \quad I_g \in \mathbb{R}^{H \times W}.$$

Next, we remove all entirely black rows and columns to extract the significant region $I' \subseteq I_g$:

$$I' = I_g[\text{rows}(I_g) \neq 0, \text{cols}(I_g) \neq 0].$$

We then pad I' appropriately to standardize its dimensions and apply resizing to reduce the spatial resolution, yielding I_r . To enhance structural coherence, Gaussian smoothing is performed:

$$I_s = \text{GaussianBlur}(I_r).$$

Finally, we binarize the image I_s to produce a binary representation I_b :

$$I_b(x, y) = \begin{cases} 1, & I_s(x, y) \neq 0 \\ 0, & \text{otherwise} \end{cases}.$$

The resulting binary matrix I_b represents navigable spaces and obstacles explicitly, serving as input for subsequent spatial reasoning tasks.

B.2. Sampling

To increase task complexity beyond uniform selection, we employ a strategy for sampling the start and target positions. For a given start cell s and any candidate cell c , the Manhattan distance is defined as

$$d(c) = |i_s - i_c| + |j_s - j_c|.$$

Let d_{\min} and d_{\max} be the minimum and maximum distances from s to all candidate cells, respectively, and normalize the distance as

$$\hat{d}(c) = \frac{d(c) - d_{\min}}{d_{\max} - d_{\min}},$$

with the convention $\hat{d}(c) = 0$ when $d_{\max} = d_{\min}$.

Given a distance weight $\alpha \in [0, 1]$, we compute the weight for each candidate as

$$w(c) = \alpha \hat{d}(c) + (1 - \alpha).$$

Then, the probability of selecting cell c is

$$P(c) = \frac{w(c)}{\sum_{c' \in C} w(c')},$$

where C is the set of candidate cells. This approach biases the selection towards cells farther from s as α increases, while still preserving an element of randomness. In our implementation, we set $\alpha = 0.5$.

C. More Discussion

It is worth noting that in the NeurIPS 2024 paper [?], the tasks are significantly simpler, involving small grid maps with only a single possible route and support for only four movement directions. This setting can be considered a strict subset of our case. Despite the simplicity, their reported navigation SR and CR using GPT-4 are only around 15% and 40%, respectively. We attribute this to the lack of a well-structured and standardized task formulation. Their outputs often contain additional words beyond the intended answer, requiring substring matching for evaluation. In contrast, our task employs a formalized output format, akin to those used in modern LLM-based planning agents, ensuring a more standardized and structured approach to path generation, and hence can be more easily applied to real-world scenarios.

D. Epilogue: Deep Reinforcement Learning

Readers familiar with AI agents trained using reinforcement learning (RL) for dynamic path navigation are aware well of the fact that, given sufficient training data, ballmark success rate (SR) for deep RL in simulated environments may exceed 0.9 with proximal policy optimization and soft actor-critic algorithms, depending on the complexity of the environment which may be cluttered with other dynamic obstacles. Our zero-shot SR and related performances, as shown in Figures 3 and 4 in the main paper, can reach this performance with typical performances above 75% in multi-turn navigation.

With no training data, we have the same performance because we are zero-shot, while the ballmark SR for deep RL will drop close to zero when it relies on exploration to learn optimal policies, which can be extremely time-consuming to even discover basic navigation strategies.

Notwithstanding, as modern LLMs are trained with RLHF, it will be an interesting and worthwhile future work to incorporate deep RL, now possible with much less training data, into our work, to gain deeper insight on LLM and deep RL integration for dynamic path navigation while further improving performance.